

C. Brunini, F. Azpilicueta, M. Gende, E. Camilion, and E. Gularte

**Abstract**

The IAG Sub-Commission 1.3b, SIRGAS (Sistema de Referencia Geocéntrico para las Américas), operates a service for computing regional ionospheric maps based on GNSS observations from its Continuously Operating Network (SIRGAS-CON). The ionospheric model used by SIRGAS (named La Plata Ionospheric Model, LPIM), has continuously evolved from a “thin layer” simplification for computing the vTEC distribution to a formulation that approximates the electron density (ED) distributions of the E, F1, F2 and top-side ionospheric layers.

This contribution presents the newest improvements in the model formulation and validates the obtained results by comparing the computed vTEC to experimental values provided by the ocean altimetry Jason 1 mission. Comparisons showed a small underestimation of the Jason 1 vTEC by about 1.3 TECu on average and rather small differences ranging from  $-0.5$  to  $-3.4$  TECu (at 95 % probability level). The results are encouraging given that comparisons were made in the open ocean regions (far away from the SIRGAS-CON stations).

**Keywords**

Ionosphere • GNSS • SIRGAS

**1 Introduction**

Not long ago, the IAG Sub-Commission 1.3b called SIRGAS (Sistema de Referencia Geocéntrico para las Américas), i.e. the Regional Reference Frame for Central and South America, operates a service for computing regional ionospheric maps based on the GNSS observations

provided by its Continuously Operating Network (SIRGAS-CON) (Brunini et al. 2011a). Since 2008, a continuous time series of maps describing the vertical Total Electron Content (vTEC) distribution for the SIRGAS region, with time resolution of 1 h, is available at the SIRGAS web page ([www.sirgas.org](http://www.sirgas.org)).

As other vTEC maps computed within the geodetic community (e.g.: Hernández-Pajarez et al. 2009), SIRGAS maps were originally based on the so called thin layer ionospheric model (Brunini et al. 2011b). According to this model, the vertical structure of the ionosphere (from about 50 to 1,000 km above the Earth’s surface), is approximated with a spherical shell of infinitesimal thickness with equivalent vTEC (located somewhere between 350 and 450 km height). Within this approximation, the satellite-to-receiver slant Total Electron Content (sTEC) is converted into an equivalent vTEC on the shell, by means of a geometrical mapping function that only depends on the satellite elevation and the

C. Brunini (✉) • F. Azpilicueta • E. Camilion • E. Gularte  
GESA, Facultad de Ciencias Astronómicas y Geofísicas, Universidad Nacional de La Plata, Paseo del Bosque s/n, La Plata 1900, Argentina  
e-mail: [claudiobrunini@yahoo.com](mailto:claudiobrunini@yahoo.com)

M. Gende  
GESA, Facultad de Ciencias Astronómicas y Geofísicas, Universidad Nacional de La Plata, Paseo del Bosque s/n, La Plata 1900, Argentina

Consejo Nacional de Investigaciones Científicas y Técnicas, Buenos Aires, Argentina

height of the shell. Spatial and temporal variations of the equivalent vTEC are represented on the shell by means of different kinds of 3-D (latitude, longitude and time) mathematical functions (e.g.: spherical harmonics expansion). The parameters of these functions are estimated from the GNSS observations, along with the inter frequency biases (IFB) that account for the frequency-dependent delays produced by the GNSS satellite and receiver hardware and firmware.

The ionospheric model used by SIRGAS, known as La Plata Ionospheric Model (LPIM) (Azpilicueta et al. 2005), has continuously evolved from the initial “thin layer with equivalent vTEC” simplification, to the present formulation in which the E, F1, F2 and top-side ionospheric layers are considered, and their vertical electron density (ED) distributions are approximated with empirical functions in similar way than the International Reference Ionosphere (IRI) (Bilitza and Reinisch 2008) or NeQuick (Nava et al. 2008) models.

At present, the SIRGAS ionospheric model is based on the geometry free observable computed from dual frequency carrier phase observations (Ciraolo et al. 2007) collected from either, ground-based or space-borne GNSS receivers on low Earth orbiting satellites (e.g.: SAC-C, GRACE, FORMOSAT-3 /COSMIC). After correcting carrier phase cycle slips and ambiguities, the geometry free observations are used (in connection with the geometrical description of the observed satellite-to-receiver line of sights; LOS) to estimate the parameters of the empirical functions that describe the 4-D (latitude, longitude, height and time) ED distribution of the different ionospheric layers. Satellite and receivers IFB are also estimated together with the function parameters.

The combination of GNSS observations collected from the Earth (with prevailing vertical LOS geometry) and from LEO (with prevailing horizontal LOS geometry) helps to solve the horizontal and vertical structure of the ED distribution (Hernández-Pajares et al. 2000).

The evolution of the SIRGAS ionospheric model has been reported in Brunini et al. (2011a) and (2011b). Those papers may be useful to clarify some points that are briefly presented in the following two sections. This contribution presents the newest improvements in the model formulation and validates the output of the model by comparing to experimental values provided by the ocean altimetry Jason 1 mission.

## 2 Model Formulation

A simple vertical ED profile is predicted by the Chapman theory (Chapman 1931), which assumes monochromatic radiation, photoionization of a single species neutral gas, and neglects transport processes:

$$N(h) = N_m \cdot \exp[k \cdot (I - z - \exp(-z))] \\ z = \frac{h - h_m}{H}, \quad (37.1)$$

where  $N(h)$  is the ED at a given height  $h$ ,  $N_m$  and  $h_m$  are the ED and height of the peak of the Chapman function, and  $H$  is the scale height. Depending on the description of electron loss process, the factor  $k$  can be 0.5 or 1, defining respectively an  $\alpha$  or  $\beta$  Chapman layer. According to Bilitza (2002), most modellers have found 0.5 to provide a closer match with observations and, according to that experience, 0.5 is used in the case of SIRGAS. In order to adapt the model to the different chemical and physical properties prevailing in the different ionospheric layers, SIRGAS uses four Chapman functions (37.1) with different parameters  $N_{m,i}$ ,  $h_{m,i}$ , and  $H_i$ ,  $i = 1, \dots, 4$ , to represent the E and F1 layers, the bottom-side of the F2 layer and the top-side:

$$N(h) = \begin{cases} \sum_{i=1}^3 N_i(h), & \text{if } h \leq h_{m,3} \\ N_4(h), & \text{if } h > h_{m,3} \end{cases}. \quad (37.2)$$

The ED,  $N_{m,3}$ , and height,  $h_{m,3}$ , of the F2 layer peak are computed from the corresponding critical frequency,  $f_3$ , and propagation factor,  $M_3$ . The critical frequency is converted into ED using the relation of proportionality between ED and squared critical frequency. The propagation factor is converted into height using the Dudeney (1974) formulae as modified by Bilitza et al. (1979) (which requires the use of the  $N_{m,3}/N_{m,1}$  ratio).

As other ionospheric models (e.g.: IRI or NeQuick), SIRGAS uses the Jones and Gallet (1962) mathematical technique to represent the geographical (latitude and longitude) and daily (UT) variation of the critical frequency and propagation factor of the F2 layer peak; symbolically:  $f_3(\varphi, \lambda, t; \mathbf{U}_f)$  and  $M_3(\varphi, \lambda, t; \mathbf{U}_M)$ , where  $\mathbf{U}_f$  and  $\mathbf{U}_M$  are vectors of 998 and 441 constant parameters respectively.

The critical frequencies and heights of the E and F1 layer peaks are computed according to the Comité Consultatif International des Radiocommunications (CCIR 1991) recommendations:

$$\left. \begin{aligned} N_{m,1} &= q_1 \cdot A_1 \cdot \cos^{n_1} \chi \\ h_{m,1} &= (1 + r_1) \cdot 120 \text{ km} \end{aligned} \right\} E \text{ layer} \\ \left. \begin{aligned} N_{m,2} &= q_2 \cdot A_2 \cdot \cos^{n_2} \chi \\ h_{m,2} &= 165 + (0.6 + r_2) \cdot \chi \end{aligned} \right\} F1 \text{ layer}, \quad (37.3)$$

where  $\chi$  is the solar zenith angle;  $A_1$ ,  $A_2$ ,  $n_1$  and  $n_2$  values depend on the geographic latitude and solar activity, and  $q_1$ ,  $q_2$ ,  $r_1$  and  $r_2$  are constant parameters.

The scale heights of the E, F1 and F2 layers are computed according to the CCIR (1991) recommendations:

$$\begin{aligned} H_3 &= \frac{(1+s_1) \cdot 38.5 \cdot N_{m,3}}{\exp[-15.2+2.0 \cdot (\ln(N_{m,3}) + \ln(M_3))]} \\ H_2 &= (I+s_2) \cdot 0.4 \cdot (h_{m,3} - h_{m,1}) \\ H_1 &= (0.5 + s_3) \cdot (5.0 + h_{m,3} - h_{m,1}) \end{aligned} \quad (37.4)$$

being  $s_1$ ,  $s_2$  and  $s_3$  constant parameters.

The top-side profile of the SIRGAS model is represented with an  $\alpha$ -Chapman function with height-varying scale height,  $H_4(h)$  (Reinisch and Huang 2001):

$$\begin{aligned} N_4(h) &= N_{m,3} \cdot \sqrt{\frac{H_4(h_{m,3})}{H_4(h)}} \times \\ &\exp\left[\frac{I}{2} \cdot [I - z_4(h) - \exp(-z_4(h))]\right], \\ z_4(h) &= \int_{h_6}^h \frac{d\zeta}{H_4(\zeta)}, \\ H_4(h) &= H_4(h_T) + \frac{H_4(h) - H_4(h_T)}{\tanh(p)} \times \\ &\tanh\left(p \cdot \frac{h - h_T}{h_{m,3} - h_T}\right), \end{aligned} \quad (37.5)$$

$h_T$  is the transition height where the dominant ion species changes from O+ to H+, and  $p$  is a steepness parameter of the topside profile.

In summary, the SIRGAS ED profile is given by a function that depends on three sets of constant but unknown parameters: 1,000 in the vector  $\mathbf{U}_N$  (including  $q_1$ , and  $q_2$ ) and 443 in the vector  $\mathbf{U}_h$  (including  $r_1$  and  $r_2$ ), needed to compute the ED and heights of the E, F1 and F2 layer peaks; and 5 parameters in the vector  $\mathbf{U}_H = (s_1, s_2, s_3, h_T, p)^T$ , required to compute the scale heights of the different layers. Symbolically, the ED profile at any point (latitude longitude and height) within the global ionosphere, and at any time (UT), is:

$$N(\varphi, \lambda, h, t; \mathbf{U}_N, \mathbf{U}_h, \mathbf{U}_H). \quad (37.6)$$

### 3 Data Assimilation

The observation equation for the problem reads as:

$$l + \varepsilon = sTEC + \beta_S + \beta_R, \quad (37.7)$$

where  $l$  is the geometry free observable from dual frequency carrier phase observations (collected from either, ground-based or space-borne GNSS receivers), already corrected by

carrier phase cycle slips and ambiguities;  $\varepsilon$  is the observational error;  $sTEC$  is a function to be estimated; and  $\beta_S$  and  $\beta_R$  are the satellite and receiver IFB.

In terms of the expression (37.6), the  $sTEC$  function of Eq. 37.7 is written as:

$$sTEC = \int_{\Gamma} N(\varphi, \lambda, h, t; \mathbf{U}_N, \mathbf{U}_h, \mathbf{U}_H) \cdot d\Gamma, \quad (37.8)$$

where, is the LOS from the satellite to the ground-based or space-borne receiver.

The function given in expression (37.6) is approximated with a linear expansion (with respect to the model parameters):

$$\begin{aligned} N(\varphi, \lambda, h, t; \mathbf{U}_N, \mathbf{U}_h, \mathbf{U}_H) &= N(\varphi, \lambda, h, t)|_0 + \\ &\frac{\partial N}{\partial \mathbf{U}_N}|_0 \cdot \Delta \mathbf{U}_N + \frac{\partial N}{\partial \mathbf{U}_h}|_0 \cdot \Delta \mathbf{U}_h + \frac{\partial N}{\partial \mathbf{U}_H}|_0 \cdot \Delta \mathbf{U}_H \end{aligned} \quad (37.9)$$

where the notation  $\cdot|_0$  is used to indicate evaluation of the function in the a-priori values of the  $\mathbf{U}_N$ ,  $\mathbf{U}_h$  and  $\mathbf{U}_H$  parameters and the symbol  $\Delta \cdot$  denotes correction to the corresponding a-priori value.

Finally, Eq. 37.7 is transformed into:

$$\begin{aligned} l + \varepsilon &= sTEC|_0 + \Delta \mathbf{U}_N \cdot \int_{\Gamma} \frac{\partial N}{\partial \mathbf{U}_N}|_0 \cdot d\Gamma + \\ &\Delta \mathbf{U}_h \cdot \int_{\Gamma} \frac{\partial N}{\partial \mathbf{U}_h}|_0 \cdot d\Gamma + \Delta \mathbf{U}_H \cdot \int_{\Gamma} \frac{\partial N}{\partial \mathbf{U}_H}|_0 \cdot d\Gamma + \beta_S + \beta_R \end{aligned} \quad (37.10)$$

where  $sTEC|_0 = \int_{\Gamma} N(\varphi, \lambda, h, t)|_0 \cdot d\Gamma$ .

Around  $5 \times 10^5$  observations per hour provided by  $\sim 200$  SIRGAS-CON stations and  $5 \times 10^3$  observations per hour derived from  $\sim 250$  FORMOSAT-3/COSMIC radio occultations per day (over the SIRGAS region) are assimilated into the SIRGAS ionospheric model. The Least Square method is used to estimate daily sets of 1,000 ( $\mathbf{U}_N$ ) + 443 ( $\mathbf{U}_h$ ) + 5 ( $\mathbf{U}_H$ ) model parameters, plus 31 IFB for the GPS satellites, plus  $\sim 200$  IFB for the SIRGAS-CON receivers plus 6 IFB for the GPS receivers flying onboard the FORMOSAT-3/COSMIC satellites (Rocken et al. 2000).

### 4 Results

A complete year from November 1, 2006, to October 31, 2007, was processed in order to assess the performance of the SIRGAS model under low solar activity conditions.

Just to provide an example, Fig. 37.1 shows the computed electron density distribution for the fixed longitude of  $60^\circ$ W and fixed UT of 14 h, from  $-55^\circ$  to  $+35^\circ$  of geographic

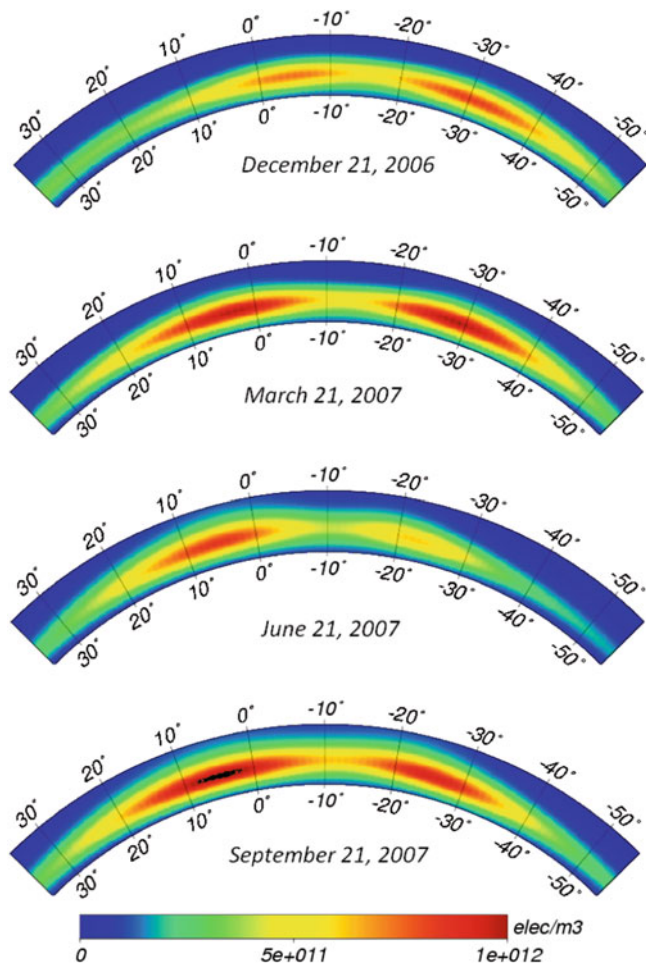


**Fig. 37.1** Electron density distribution for fixed longitude and UT (60°W, 14 h), from  $-55^\circ$  to  $+35^\circ$  of geographic latitude and from 50 to 1,000 km height

latitude and from 50 to 1,000 km height, for the two solstices and equinoxes comprised in the analysed period. Seasonal changes in the morphology of the Appleton Anomaly are quite well represented by this figure.

In order to assess the accuracy of the obtained results, the vTEC distribution computed by integration of the SIRGAS ED distribution, is compared to experimental vTEC values derived from the dual frequency radar onboard the Jason 1 satellite altimetry mission (Menard and Haines 2001).

All Jason 1 observations for the whole year, within the ocean region surrounding the Latin America continent, from  $0^\circ$  to  $120^\circ$  W longitude and  $+40^\circ$  to  $-60^\circ$  modip latitude, are considered. In order to reduce the computational load, normal points every 30s are computed from the original 1 s sampling rate observations.

The SIRGAS vTEC is computed for the time and location of every smoothed Jason 1 vTEC, by integration of the ED up to the height of the Jason 1 satellite

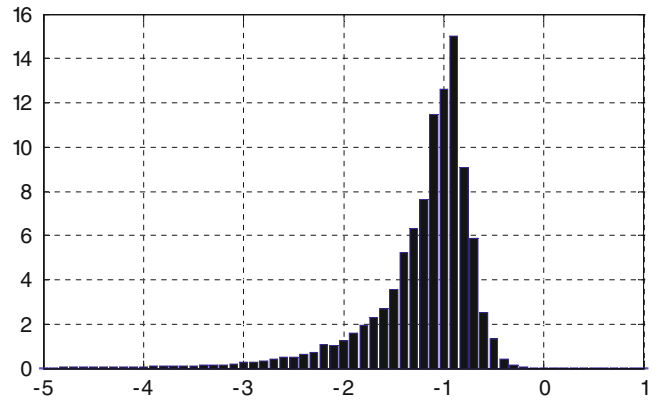


**Fig. 37.2** Distribution of differences SIRGAS minus Jason 1 vTEC (x-value in TECu and y-value in percent)

( $\sim 1,300$  km). Then, the differences SIRGAS minus Jason 1 vTEC are evaluated.

The mean value of the differences for the whole year is  $-1.3$  TECu, meaning that the SIRGAS model slightly underestimates the Jason 1 vTEC. According to Fig. 37.2, 95 % of the differences range from  $-0.5$  to  $-3.4$  TECu with a statistical distribution biased toward negative values.

Figure 37.3 shows a set of maps displaying the differences SIRGAS minus Jason 1 vTEC for the whole year, grouped into UT intervals of 2 h. The dashed lines represent the modip parallels of  $+30^\circ$ ,  $0^\circ$ ,  $-30^\circ$  and  $-60^\circ$ . Within the mid latitude region ( $|modip| > 30^\circ$ ) the differences stay very small (in absolute value), even far from the continent. Their values slightly increase in the low latitude region ( $|modip| \leq 30^\circ$ ) for the UT intervals when the Appleton Anomaly deploys over Latin America.

## 5 Conclusions

SIRGAS vTEC was compared to the corresponding values provided by the Jason 1 satellite altimetry mission, for a complete low solar activity year. According to this comparison, there is a bias of  $-1.3$  TECu on average between the SIRGAS and Jason 1 vTEC (SIRGAS lower than Jason 1). This bias is compatible with other results reported in the literature regarding systematic differences between the vTEC estimated from GPS and from Jason 1–2 and TOPEX (Codrescu et al. 2001; Hernandez-Pajares 2003; Delay and Doherty 2004; Brunini et al. 2005). In fact, in a previous paper we pointed out the possibility that the TOPEX-GPS bias could be partially attributed to calibration errors on the TOPEX system biases.

Differences SIRGAS minus Jason 1 vTEC are very small (95 % differences range from  $-0.5$  to  $-3.4$  TECu). Within the mid latitude region the differences stay small even far



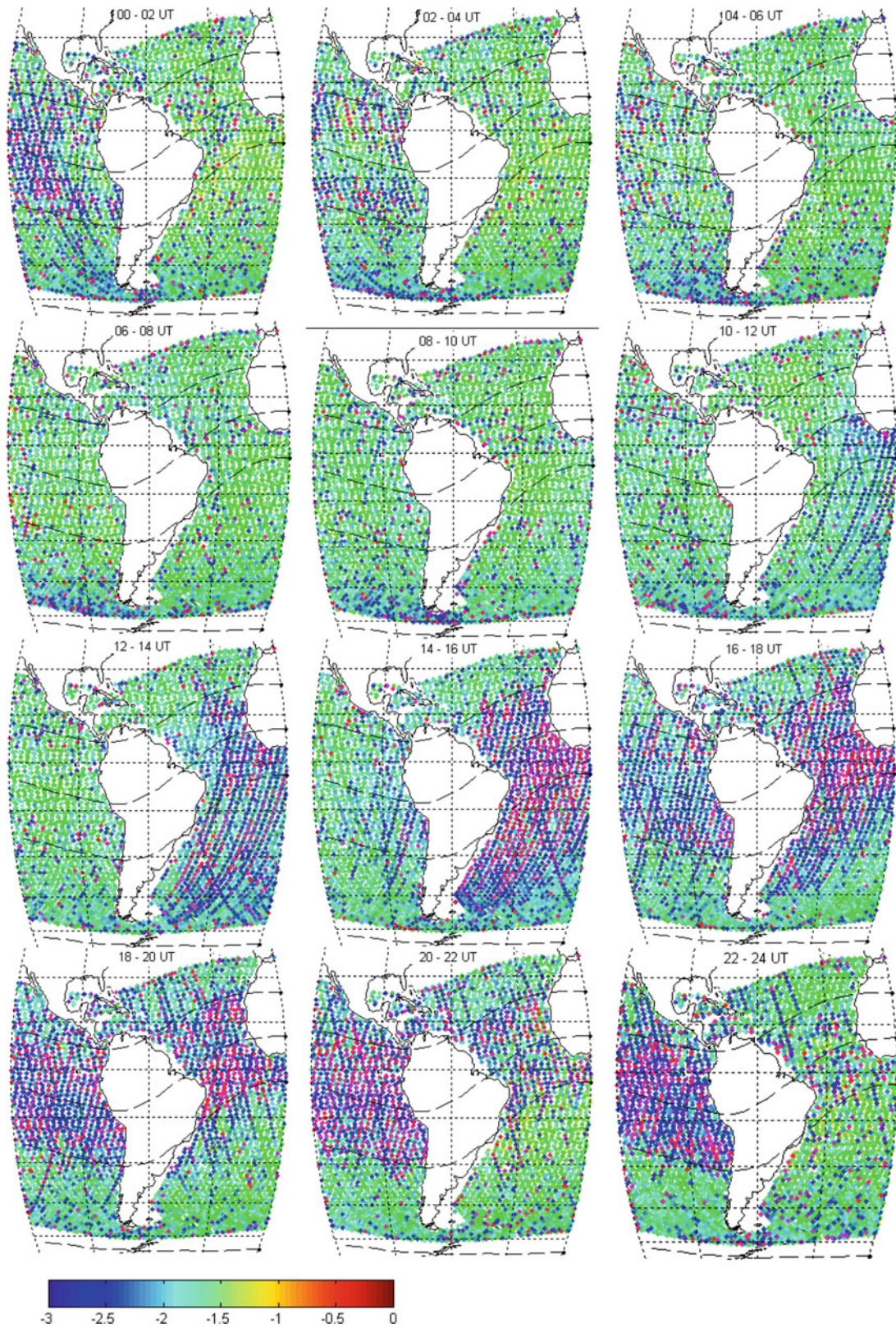


**Fig. 37.3** Differences SIRGAS minus Jason 1 vTEC (TECu) for different UT intervals

from the continent, where SIRGAS-CON stations are not available. Their values slightly increase in the low latitude region for the UT intervals when the Appleton Anomaly evolves over the Latin American continent, but 95 % of the samples stay within (0, -3.5) TECu.

The obtained results are considered very encouraging, overall because they were obtained in open ocean regions where ground-based observations are inexistent and the model relies only on FORMOSAT-3/COSMIC observations.

## References

- Azpilicueta F, Brunini C, Radicella SM (2005) Global ionospheric maps from GPS observations using modip latitude. *Adv Space Res* 38(11):2324–2331
- Bilitza D (2002) Ionospheric models for radio propagation studies. Chapter 28. In: W. Ross Stone (ed.) *The Review of Radio Science 1999–2002*. Wiley Interscience, ISBN 0-471-26866-6, pp 625–679
- Bilitza D, Reinisch BW (2008) International reference ionosphere 2007: improvements and new parameters. *Adv Space Res* 42(4): 599–609
- Bilitza D, Sheik NM, Eyfrig R (1979) A global model for the height of the F2-peak using M3000 values from CCIR. *Telecommun J* 46:549–553
- Brunini C, Azpilicueta F, Gende M, Aragón-Ángel A, Hernández-Pajares M, Juan JM, Sanz J (2011a) Toward a SIRGAS service for mapping the ionosphere's electron density distribution. In: Pacino C et al. (eds) *Geodesy for planet earth, IAG symposia*, vol 135, Buenos Aires, Argentina, 31 August 31 – 4 September 2009, pp. 575–580, ISBN 978-3-642-20338-1, Springer
- Brunini C, Azpilicueta F, Gende M, Camilion E, Aragón Ángel A, Hernandez-Pajares M, Juan M, Sanz J, Salazar D (2011b) Ground- and space-based GPS data ingestion into the NeQuick model. *J Geod* 18(12):931–939
- Brunini C, Sánchez L, Drewes H, Costa S, Mackern V, Martínez W, Seemüller W, da Silva A (2011c) Improved analysis strategy and accessibility of the SIRGAS Reference Frame. In: Pacino C et al. (eds) *Geodesy for planet Earth, IAG symposia*, vol 135, Buenos Aires, Argentina, 31 August 31 – 4 September 2009, pp 3–8, ISBN 978-3-642-20338-1, Springer
- Brunini C, Meza A, Bosch W (2005) Temporal and spatial variability of the bias between TOPEX and GPS derived TEC. *J Geod* 79:175–188. doi:10.1007/s00190-005-0448-z
- CCIR (1991) Report 340–6. Comité Consultatif International des Radio communications, Genève, Switzerland
- Chapman S (1931) The absorption and dissociative or ionizing effect of monochromatic radiation in an atmosphere on a rotating Earth. In: *Proceedings of the physical society*, vol 43, pp 483–501. doi:10.1088/0959-5309/43/5/302.
- Ciraolo L, Azpilicueta F, Brunini C, Meza A, Radicella SM (2007) Calibration errors on experimental slant total electron content determined with GPS. *J Geod* 81(2):111–120
- Codrescu MV, Beierle KL, Fuller-Rowell TJ (2001) More total electron content climatology from TOPEX/Poseidon measurements. *Radio Sci* 36(2):325–333
- Delay S, Doherty P (2004) A decade of ionospheric measurements from the TOPEX/Poseidon mission. Contribution to the International Beacon Satellite Symposium, Trieste, October 18–22
- Dudney JR (1974) A simple empirical method for estimating the height of the F2-layer at the Argentine Islands Graham Land. Science report no. 88, London, British Antarctic Survey
- Hernandez-Pajares M (2003) Performance of IGS ionosphere TEC maps. Presented at 22nd IGS Governing Board Meeting, Nice, 6 April 2003
- Hernández-Pajares M, Juan JM, Sanz J (2000) Improving the Abel inversion by adding ground GPS data to LEO radio occultations in ionospheric sounding. *Geophys Res Lett* 27(16):2473–2476
- Hernández-Pajares M, Juan JM, Sanz J, Orus R, Garcia-Rigo A, Feltens J, Komjathy A, Schaer SC, Krankowski A (2009) The IGS VTEC maps: a reliable source of ionospheric information since 1998. *J Geod* 83:263–275
- Menard Y, Haines B (2001) Jason-1 CALVAL plan, JPL Ref: TP2-J0-PL-974-CN (PO.DAAC)
- Nava B, Coisson P, Radicella SM (2008) A new version of the NeQuick ionosphere electron density model. *J Atmos Sol Terr Phys*. doi:10.1016/j.jastp.2008.01.015, 1856-1862
- Reinisch BW, Huang X (2001) Deducing topside profiles and total electron content from bottomside ionograms. *Adv Space Res* 27(1):23–30
- Rocken C, Kuo YH, Schreiner W, Hunt D, Sokolovsky S (2000) COSMIC system description. *Spec Iss Terr Atmos Ocean Sci* 11(1):21–52